Hindawi Publishing Corporation
Advances in Mathematical Physics
Volume 2015, Article ID 437869, 9 pages
http://dx.doi.org/10.1155/2015/437869

Research Article

Coupling Influence on Signal Readout of a Dual-Parameter LC Resonant System

Jijun Xiong,[1,2] Tanyong Wei,[1,2] Tao Luo,[1,2] Qiulin Tan,[1,2,3] Chenyang Xue,[1,2] Jun Liu,[1,2] and Wendong Zhang[1,2]

[1]*Key Laboratory of Instrumentation Science & Dynamic Measurement, Ministry of Education, North University of China, Tai Yuan 030051, China*
[2]*Science and Technology on Electronic Test & Measurement Laboratory, North University of China, Tai Yuan 030051, China*
[3]*State Key Laboratory of Transducer Technology, Department of Precision Instrument and Mechanology, Tsinghua University, Beijing 10084, China*

Correspondence should be addressed to Jijun Xiong; xiongjijun@nuc.edu.cn and Qiulin Tan; tanqiulin@nuc.edu.cn

Received 1 February 2015; Accepted 3 May 2015

Academic Editor: Mikhail Panfilov

Dual-parameter inductive-capacitive (LC) resonant sensor is gradually becoming the measurement trend in complex harsh environments; however, the coupling between inductors greatly affects the readout signal, which becomes very difficult to resolve by means of simple mathematical tools. By changing the values of specific variables in a MATLAB code, the influence of coupling between coils on the readout signal is analyzed. Our preliminary conclusions underline that changing the coupling to antenna greatly affects the readout signal, but it simultaneously influences the other signal. When $f_{01} = f_{02}$, it is better to broaden the difference between the two coupling coefficients k_1 and k_2. On the other side, when f_{01} is smaller than f_{02}, it is better to decrease the coupling between sensor inductors k_{12}, in order to obtain two readout signals averaged in strength. Finally, a test system including a discrete capacitor soldered to a printed circuit board (PCB) based planar spiral coil is built, and the readout signals under different relative inductors positions are analyzed. All experimental results are in good agreement with the results of the MATLAB simulation.

1. Introduction

A dual-parameter test is urgently needed in the fields of aviation, mining, and automation industries. In these industries, a dual-parameter test is required for specific applications such as blade temperature and pressure monitoring in turbine engines [1–3], temperature and vibration monitoring in key components of coal mining machines [4], and monitoring airflow pressure and vibration on the aircraft surface [5–7]. All these applications require proper design and functional safety of key components. Usually, several single sensors are employed, each of them dedicated to test only one parameter. However, this solution is costly, it occupies a large volume, and it may even affect the performance of original components [8]. Therefore, the development of a sensor that monitors dual parameters becomes reasonable. Several groups have started conducting research on dual-parameter sensors [9–12] in recent years. For example, the Precision Engineering Department of the Xi'jiao University has started its research on simultaneous pressure and temperature monitoring in 2006 [9], employing semiconductor Silicon technology. Nonetheless, silicon technology requires wire connection and can only operate up to 250°C, because of drastically increased leakage currents across the junction at elevated temperatures. The team led by Professor Albert P. Pisano started its research on blade temperature and pressure monitoring in gas engines in 2009 [10], based on the dual-LC resonant sensor. This technology showed great potential, because it could wirelessly measure multiple parameters without the need for a battery.

The LC resonant sensor is a passive, wireless, easy-to-machine, adaptable to harsh environment [13, 14] sensor,

based on a magnetic coupling readout method and combined with a ceramic micropackage technology. Dual LC circuits are usually integrated into a chip; however, changes in the coupling coefficient or in the LC circuit parameters influence the readout signal quality, which in turn affect the sensor-readout distance, as well as the sensor working temperature [15]. Therefore, it is important to analyze the coupling influence on the readout signal from a theoretical point of view, in order to build a foundation for the design and fabrication of an optimized dual-LC resonant sensor.

We first introduce the single-parameter test concept. Then, we focus on the theory of dual LC circuits. Using the MATLAB software, the effect of changing either the coupling coefficient or the LC circuit parameters on the readout signal is analyzed. Finally, a test-system including a discrete capacitor soldered to a PCB based planar spiral coil is developed, and the sensor readout signal is analyzed under different relative positions among the coils. All experimental results are in agreement with the simulation results.

2. Single-Parameter Test

As shown in Figure 1, to interrogate the sensor, a loop-antenna with inductance L_0 is magnetically coupled to an inductance L_1. The loop-antenna sends out an alternating current sweep frequency signal of a certain bandwidth. Using the transformer network theory and Kirchhoff law, the input impedance Z_{in} looking into the antenna is given by [16]

$$Z_{\text{in}} = R_0 + jwL_0 + \frac{(wM)^2}{jwL_1 + R_1 + 1/jwC_1}, \tag{1}$$

$$M = k\sqrt{L_0L_1}, \tag{2}$$

$$w = 2\pi f, \tag{3}$$

where k denotes the coupling coefficient between inductors and f represents frequency of AC signal. By analyzing (1), a simple equation for f_{min}, the minimum measured frequency extracted from the impedance-phase curve is obtained [17] as

$$f_{\text{min}} = f_0\left(1 + \frac{k^2}{4} + \frac{1}{8Q^2}\right), \tag{4}$$

where Q denotes the LC circuit quality factor, while f_0 is the self-resonant frequency and is defined below as

$$f_0 = \frac{1}{2\pi\sqrt{L_1C_1}}. \tag{5}$$

The equation for Z_{in} is analyzed using the MATLAB software. Values for the initialized variables are listed in Table 1.

The coupling coefficient k in Table 1 is varied from 0.1 to 0.3, with a 0.05 step length. The other variables are kept constant. As shown in Figure 2, the minimum measured frequency f_{min} shifts rightward with a corresponding decreased phase dip Φ_{min}, while the frequency band is clearly broadened. For $k = 0.2$, the measured f_{min} is 20.74 MHz,

Table 1: Initial values of the antenna and the LC circuit.

L_0 (μH)	R_0 (Ω)	L_1 (μH)	R_1 (Ω)	C_1 (pF)	k
1.5	3	6	3	10	0.1 : 0.05 : 0.3

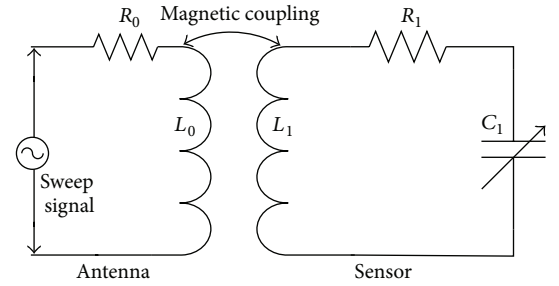

Figure 1: Schematic diagram of the single-parameter LC resonant sensor system.

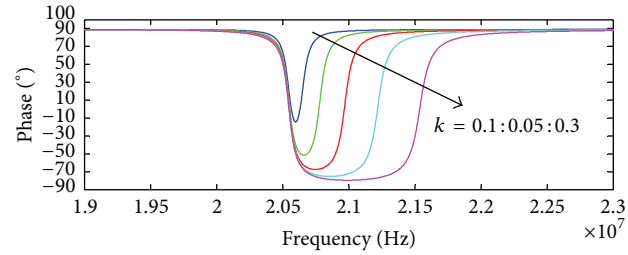

Figure 2: Change of coupling coefficient k as a function of frequency.

Φ_{min} is equal to −67.5°, while the self-resonant frequency f_0 is calculated to be 20.54 MHz. The difference between f_{min} and f_0 is found to be very small.

3. Dual-Parameters Test

As shown in Figure 3, the antenna is coupled with two LC circuits. The added LC circuit results in two additional couplings. Similar to the single-parameter test, the transformer network theory and Kirchhoff law are used, and the input impedance Z_{in} looking into the antenna is given by [18]

$$Z_{\text{in}} = R_0 + jwL_0 + jwM_1\frac{-w^2M_2M_{12} - jwM_1Z_2}{Z_1Z_2 + w^2M_{12}^2} + jwM_2\frac{-w^2M_1M_{12} - jwM_2Z_1}{Z_1Z_2 + w^2M_{12}^2}, \tag{6}$$

where

$$M_1 = k_1\sqrt{L_0L_1},$$

$$M_2 = k_2\sqrt{L_0L_2}, \tag{7}$$

$$M_{12} = k_{12}\sqrt{L_1L_2}.$$

k_1, k_2, k_{12} are coupling coefficients between the antenna and inductor 1, antenna and inductor 2, and between inductors,

Table 2: Initial values for the antenna and for the two LC circuits.

L_0 (μH)	R_0 (Ω)	L_1 (μH)	R_1 (Ω)	C_1 (pF)	L_2 (μH)	R_2 (Ω)	C_2 (pF)	k_1	k_2	k_{12}
1.5	3	6	3	10	6	3	10	0.2	0.2	0.2

Table 3: C_2 change from 3 pF to 9 pF.

L_0 (μH)	R_0 (Ω)	L_1 (μH)	R_1 (Ω)	C_1 (pF)	L_2 (μH)	R_2 (Ω)	C_2 (pF)	k_1	k_2	k_{12}
1.5	3	6	3	10	6	3	3 : 2 : 9, 10 : 2 : 18	0.2	0.2	0.2

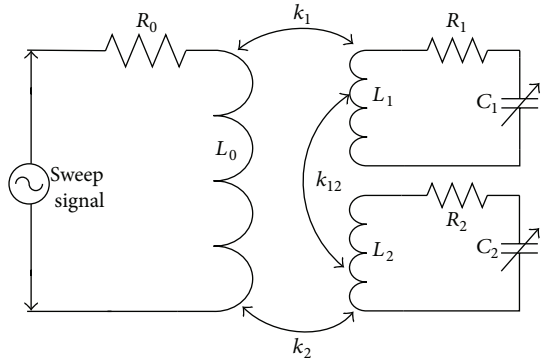

Figure 3: Test of an antenna and dual LC circuits.

respectively. Z_1 and Z_2 denote the system impedances of LC circuits 1 and 2 (Figure 3), respectively, which are defined below:

$$Z_1 = R_1 + jwL_1 + \frac{1}{jwC_1},$$
$$Z_2 = R_2 + jwL_2 + \frac{1}{jwC_2}. \quad (8)$$

As seen from (6), the impedance becomes very complicated, and it is difficult to derive the relation between $f_{\min 1}$, $f_{\min 2}$ (measured frequencies) and f_{01}, f_{02} (resonant frequencies) [18]. Using MATLAB, (6) is analyzed by initializing the variables, in order to see its influence on the final readout signal. Table 2 indicates that the variables listed in Table 1 remain even after the addition of LC circuit 2.

3.1. Change in the LC Circuit Parameters. First, capacitance C_2 shown in Table 2 is changed from 3 pF to 9 pF, with a 2 pF step, as shown in Table 3.

The simulation results are shown in Figure 4(a). While the measured frequency $f_{\min 2}$ (the right readout signal) shifts leftward, with a rapidly decreasing signal strength, the left readout signal only suffers from a slight change, simultaneously with the measured frequency $f_{\min 1}$ decreasing from 20.60 MHz to 19.49 MHz and the impedance phase $\Phi_{\min 1}$ dropping from -70.19° to -77.17°. It is found that the addition of LC circuit 2 to the coupling leads to a slight increase in the left readout signal strength, in contrast with the scenario without circuit 2 as shown in Figure 2.

Similarly, results in Figure 4(b) show a situation where capacitance C_2 is changed from 10 pF to 18 pF, with the other variables kept constant (Table 3). From Figure 4(b), we see that $f_{\min 2}$ (left readout signal) shifts leftward with a slightly increased signal strength, while the LC circuit 1 readout signal (right-hand side of the plot) clearly changes, with $f_{\min 1}$ decreasing from 22.18 MHz to 21.52 MHz and $\Phi_{\min 1}$ being enhanced from 45.83° to -32.00°. For $C_2 = 10$ pF, namely, when the parameters in the LC circuits are the same, the two readout signals merge into a single signal.

From the results shown in Figure 4, we state that in a dual-parameter test system, the change in the circuit parameter greatly affects its own readout signal, at the same time slightly influencing the other readout signal. Further, as indicated from Figure 4, when the coupling coefficients k_1 and k_2 are the same, and the more apart f_{01} is from f_{02}, the higher is the averaged value of both signal strengths.

3.2. Change of Coupling for Circuits at the Same Frequency. It has already been shown that when the parameters in LC circuits are the same, namely, $L_1 = L_2$, $C_1 = C_2$, and $k_1 = k_2$, there will be only one readout signal. Thus, in the following analysis, only the coupling coefficient k_2 in Table 2 is changed from 0.05 to 0.25, with the other variables are shown in Table 4.

The simulation results presented in Figure 5 show the situation when the coupling coefficients k_1 and k_2 are different, with the two readout signals clearly separated. With the increase in k_2, the left signal varies similarly to what is described for the single-parameter condition, mentioned in Section 2. Whereas the right signal changes simultaneously, through analysis on the right signal, it is found that the readout signal strength is stronger when k_2 is at a farther distance from k_1.

3.3. Change of Coupling for Circuits at Different Frequencies. In contrast with data presented in Table 2, in this section, the variable L_2 is changed (Table 5). In this case, the self-resonant frequency $f_{\min 2}$ derived from (5) is 29.05 MHz. Similarly, only L_2 in Table 5 is changed in order to track the influence on the readout signal in simulation.

First, variable k_{12} in Table 5 is changed from 0.1 to 0.5 with a 0.1 step, which is listed in Table 6.

From Figure 6, it is found that in this case, the readout signals move in an opposite direction to the increase in k_{12}. The left frequency $f_{\min 1}$ changes from 20.67 MHz to

Table 4: Change of k_2.

L_0 (μH)	R_0 (Ω)	L_1 (μH)	R_1 (Ω)	C_1 (pF)	L_2 (μH)	R_2 (Ω)	C_2 (pF)	k_1	k_2	k_{12}
1.5	3	6	3	10	6	3	10	0.2	0.05 : 0.05 : 0.25	0.2

Table 5: Initial value of the antenna and two LC circuits.

L_0 (μH)	R_0 (Ω)	L_1 (μH)	R_1 (Ω)	C_1 (pF)	L_2 (μH)	R_2 (Ω)	C_2 (pF)	k_1	k_2	k_{12}
1.5	3	6	3	10	3	3	10	0.2	0.2	0.2

Table 6: Change in k_{12}.

L_0 (μH)	R_0 (Ω)	L_1 (μH)	R_1 (Ω)	C_1 (pF)	L_2 (μH)	R_2 (Ω)	C_2 (pF)	k_1	k_2	k_{12}
1.5	3	6	3	10	3	3	10	0.2	0.2	0.1 : 0.1 : 0.5

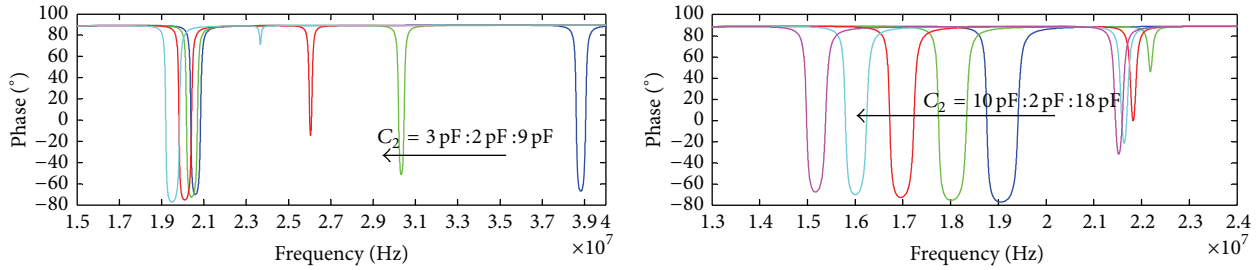

Figure 4: Simulation results upon changing C_2 from (a) 3 pF to 9 pF, (b) 10 pF to 18 pF.

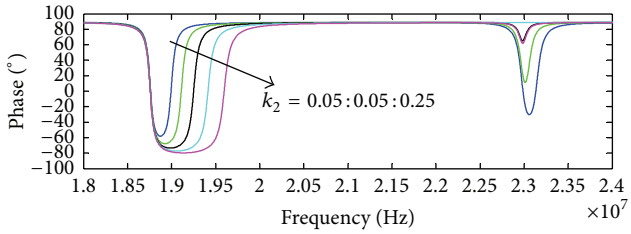

Figure 5: Simulation results upon changing k_2.

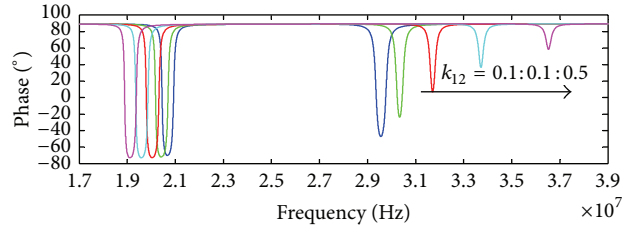

Figure 6: Simulation results upon changing k_{12}.

19.11 MHz, with a slightly decreased Φ_{min}, while the right f_{min2} increases from 29.55 MHz to 36.53 MHz, with a readout signal strength rapidly decreasing. Figure 6 shows that increasing k_{12} contributes to the separation of the two signals, and this leads to a strengthened and weakened readout signal.

The coupling coefficient k_1 in Table 5 is changed. As shown in Figure 7(a), with the decrease in k_1, the left readout signal (LC circuit 1) is changed similar to the single-parameter situation, while the right signal f_{min2} (LC circuit 2) shifts rightward 0.14 MHz with Φ_{min2} clearly strengthened from 9.09° to −45.01°.

Finally, the k_2 listed in Table 5 is also changed. As shown in Figure 7(b), with the increase in k_2, the right readout signal (LC circuit 2) is changed, similarly to the single-parameter situation; however, the left signal slightly varies, with f_{min1} increased by 0.07 MHz and Φ_{min1} enhanced by only 5°.

From what was described in Figure 7, with respect to changing k_1 and k_2, it is found that changing coupling between the LC circuit and antenna greatly affects its own readout signal, which is similar to the single-parameter situation (as stated in Section 2); however, it simultaneously influences the other readout signal. When f_{01} is smaller than f_{02}, decreasing k_1 will get an enhanced readout signal Φ_{min2}, while increasing k_2 will get a slightly strengthened Φ_{min1}.

4. Experiment and Test

The coupling coefficient has a connection with many other factors such as a spiral coil shape, position, gap, slant angle, facing area between coils, and so forth. There are many studies describing the method to exactly calculate the coupling

Table 7: Dimensions of the PCB-based planar spiral coil.

Outer dimension of inductor (mm^2)	Number of turns	Wire width (mm)	Wire spacing (mm)	Wire thickness (μm)	Substrate thickness (mm)	Substrate dimension (mm^2)
30×30	10	0.3	0.3	15	0.58	33×33

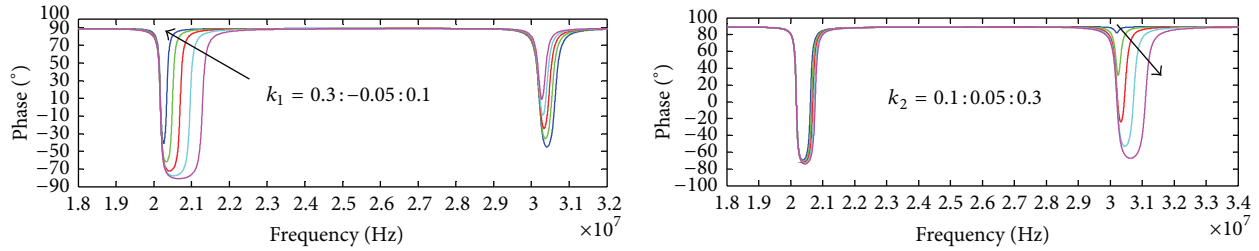

Figure 7: Simulation results upon changing (a) k_1 and (b) k_2.

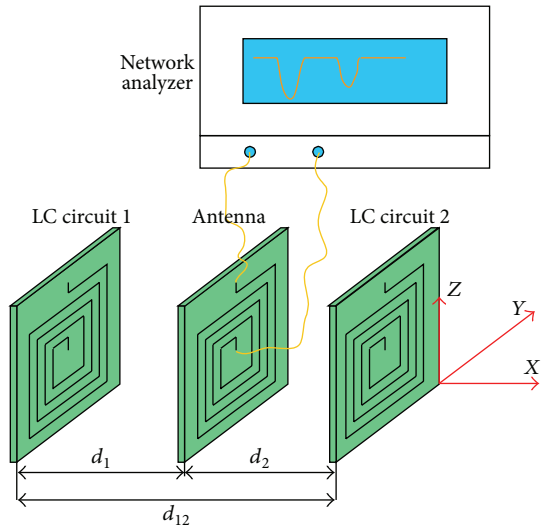

Figure 8: Relative position of three coils.

coefficient between two spiral coils in theory [19–21]; however, in our analysis, this is not required because of the complicated mathematical expressions involved. It is well known that the coupling coefficient is monotonic with the facing area and the gap between two planar spiral coils [22]; hence, for qualitative analysis, all coils in the experiment are printed on a PCB board with the same dimensions (Table 7). The LC circuit comprises a capacitor with pins soldered to the PCB board.

4.1. Relative Position 1. As visible from Figure 8, the antenna is placed in the middle and the LC circuits are positioned to the left and to the right sides of it, in perfect alignment with the antenna. Both the distances d_1 and d_2 are equal to 7 mm, to ensure $k_1 = k_2$. Capacitance C_1, soldered to the LC circuit 1 is changed from 3 pF to 9 pF and from 10 pF to 18 pF, with a step length of 2 pF, respectively, while C_2 stays fixed at 10 pF. The test result is shown in Figure 9. It is found that a strong readout signal and a weak readout signal are clearly distinguishable when C_1 deviates from C_2, whereas they merge into one signal when $C_1 = C_2$. Thus, it is better to deviate C_1 from C_2 to ensure that both signals are strengthened. The average strength of the signal when C_2 deviates from C_1 agrees with that obtained from the MATLAB simulation results.

Next, we move coil 1 leftward from 4 mm to 10 mm with a 1 mm-step, while d_2 is kept fixed at 7 mm. The capacitors soldered are both 10 pF. It is known that moving inductor 1 causes a change in both k_1 and k_{12}, but the change in k_1 is larger than the one in k_{12}. In fact, for a magnetic field, the strength is in inverse ratio with the third power of the gap [22], while d_{12} is almost twice the distance of d_1. The result is shown in Figure 10. It is found that the right signal strength gradually decreases from 4 mm to 7 mm, and it completely disappears at 7 mm. For longer distances, the right signal starts to increase again from 7 mm to 10 mm. This proves that the signal weakens when k_1 gets close to k_2, while it gets stronger when they deviate from one another. The left test signal changes similar to the single-parameter test situation.

To study the influence of different resonant frequency LC circuits on the antenna, a capacitor of 20 pF is soldered to circuit 1, while C_2 is kept at 10 pF. Coil 1 is moved leftward from 3 mm to 6 mm, while d_2 is kept at 7 mm. The readout result is shown in Figure 11(a). It is found that when f_{01} is smaller than f_{02}, the right strength (LC circuit 2) is clearly enhanced, and the left signal (LC circuit 1) varies similar to the single-parameter situation. Then, as above, coil 2 is moved leftward from 6 mm to 3 mm, while d_1 is kept at 7 mm. The test result shown in Figure 11(b) indicates that the left signal

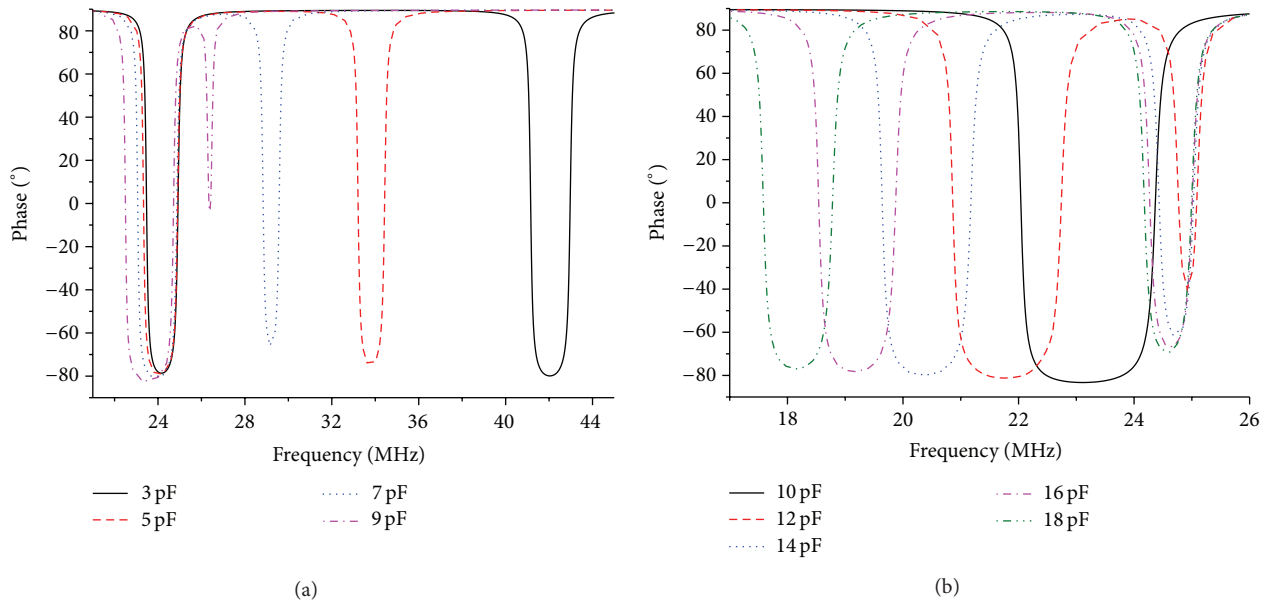

Figure 9: Test result upon changing C_1 from (a) 3 pF to 9 pF, (b) 10 pF to 18 pF.

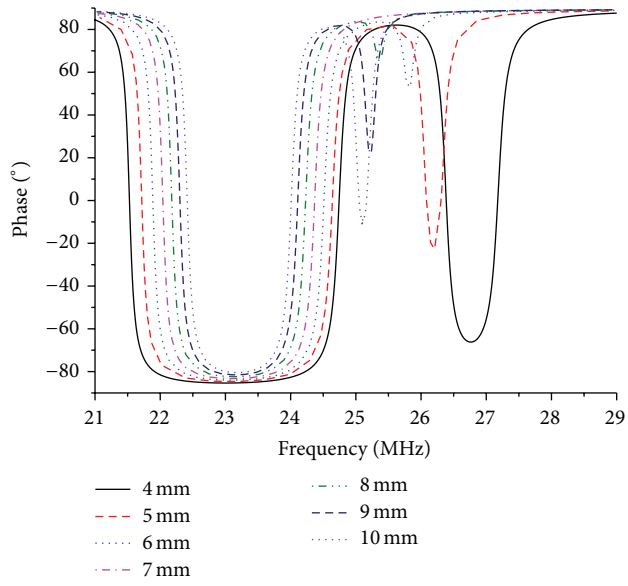

Figure 10: Test result upon moving coil 1 leftward.

is slightly enhanced differently from the situation described in Figure 11(a).

4.2. Relative Position 2. In the following configuration, the antenna is placed on the left side and three coils are in perfect mutual alignment. The capacitors soldered to the circuits are both 10 pF. Coil 2 in the experiment is moved outward from 0.5 mm to 3 mm, with a 0.5 mm step, while d_1 is kept at 7 mm. As above, both couplings k_2 and k_{12} are decreased when moving coil 2 rightward; however, k_{12} increases considerably more than k_2, for the gap d_{12} is much smaller than d_2. The result is shown in Figure 12(b). It is found that the two test signals move close to each other, which proves that decreasing k_{12} contributes to the two signals approach.

Then, as shown in Figure 13(a), coil 2 is moving in the Y-direction with a step of 7.5 mm, to gradually stagger two coils. The gaps d_{12} and d_1 are kept equal to 1 mm and 7 mm, respectively. The results are shown in Figure 13(b). It is found that at the beginning the two test signals move close to each other up to 22.5 mm, because of the decrease in the k_{12}

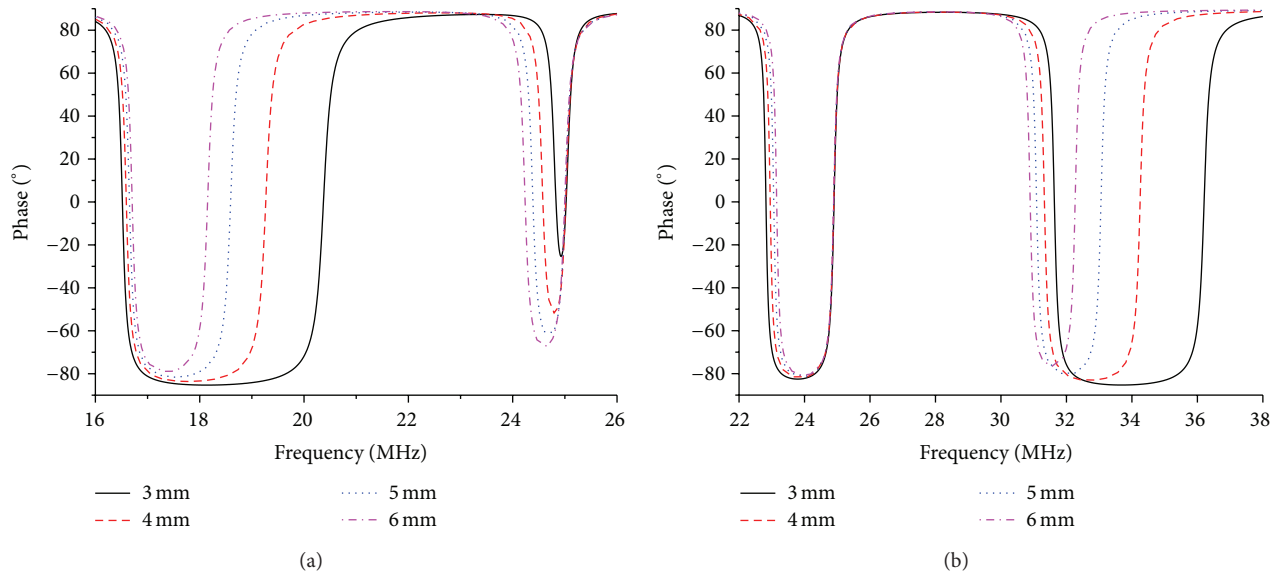

Figure 11: Test result of moving (a) coil 1 outward, (b) coil 2 inward.

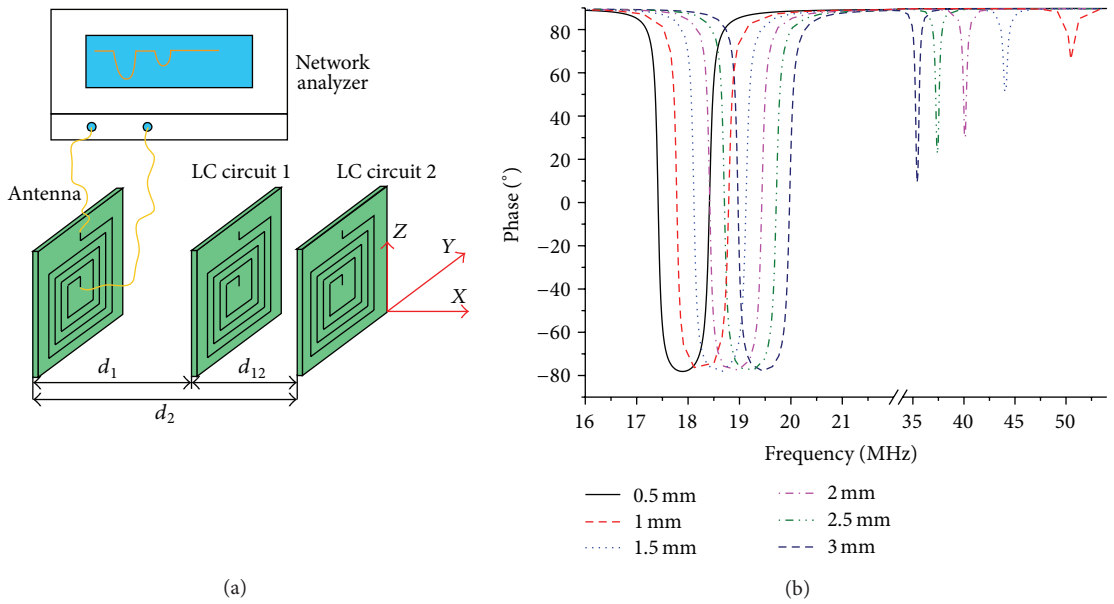

Figure 12: (a) Relative position of three coils. (b) Test result.

coupling. Next, the coupling between LC circuits becomes very weak, causing tested signals to slightly change until coil 2 gets totally away from coil 1.

5. Conclusion

This paper first introduced the theoretical model of a dual-parameter LC resonant sensor. Because of the difficulties in clearly analyzing complicate mathematical relations, a MATLAB software is used. We initialized the variables and studied the influence of changing variables on the readout signal according to different situations. Preliminarily conclusions are drawn based on the above-mentioned MATLAB tool. Finally, a test system including a discrete capacitor soldered to a PCB-based planar spiral coil is built and different relative positions among three spiral coils were researched.

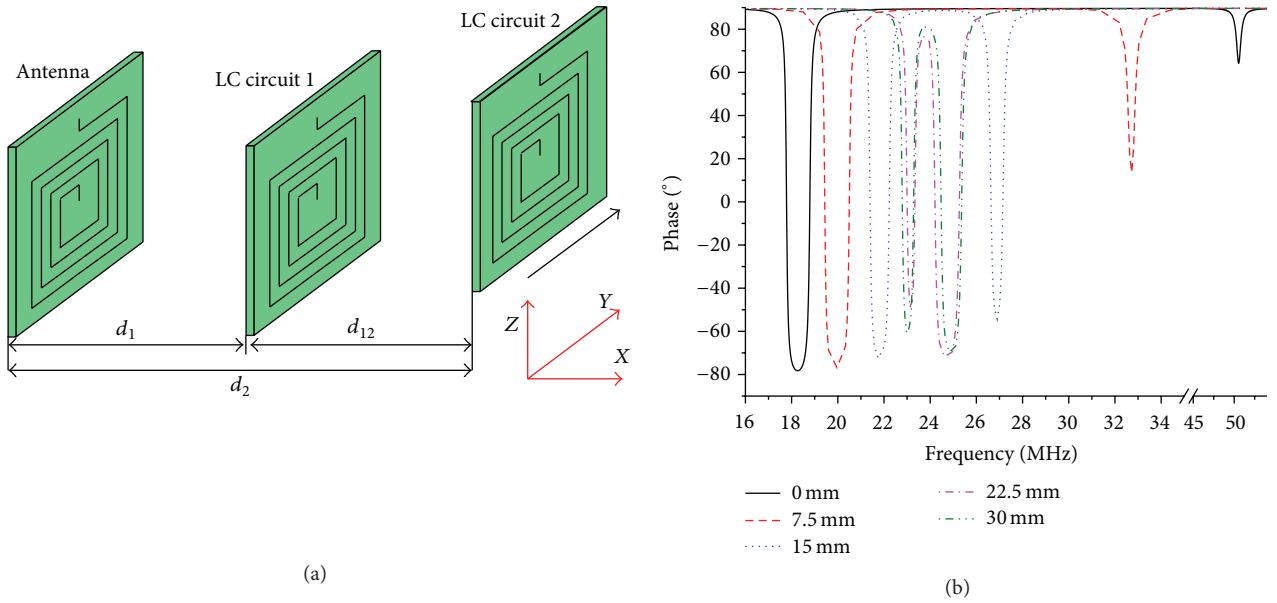

Figure 13: (a) Relative position of the three coils. (b) Test result.

All experimental results are in agreement with simulation results in MATLAB.

Conflict of Interests

The authors declare no conflict of interests.

Acknowledgments

This work was supported by the National Natural Science Foundation of China (no. 61471324), the National Outstanding Youth Fund of China (no. 51425505), the Program for the Top Young Academic Leaders of Higher Learning Institutions of Shanxi Province, China, and the Post-doctor special Foundation of Tsinghua University, China (2014T70074).

References

[1] C. M. Spadaccini, J. Lee, S. Lukachko et al., "High power density silicon combustion systems for micro gas turbine engines," in *Proceedings of Turbo Expo 2002: Power for Land, Sea, and Air*, pp. 469–481, American Society of Mechanical Engineers, 2002.

[2] A. C. Eckbreth, G. M. Dobbs, J. H. Stufflebeam, and P. A. Tellex, "CARS temperature and species measurements in augmented jet engine exhausts," *Applied Optics*, vol. 23, no. 9, pp. 1328–1339, 1984.

[3] A. Mehra, X. Zhang, A. A. Ayón, I. A. Waitz, M. A. Schmidt, and C. M. Spadaccini, "Six-wafer combustion system for a silicon micro gas turbine engine," *Journal of Microelectromechanical Systems*, vol. 9, no. 4, pp. 517–527, 2000.

[4] L. O. U. Pu-Gen and S. Wen-Ai, "Design and implementation of real-time temperature measuring and wireless transmission system under mine," *Instrument Technique and Sensor*, vol. 3, p. 17, 2007.

[5] T. J. Bruno and B. L. Smith, "Improvements in the measurement of distillation curves. 2. Application to aerospace/aviation fuels RP-1 and S-8," *Industrial and Engineering Chemistry Research*, vol. 45, no. 12, pp. 4381–4388, 2006.

[6] D. H. Lenschow, *The Measurement of Air Velocity and Temperature Using the NCAR Buffalo Aircraft Measuring System*, National Center for Atmospheric Research, 1972.

[7] V. W. Yuan, J. D. Bowman, D. J. Funk et al., "Shock temperature measurement using neutron resonance spectroscopy," *Physical Review Letters*, vol. 94, no. 12, Article ID 125504, 2005.

[8] J. Xiong, Y. Li, Y. Hong et al., "Wireless LTCC-based capacitive pressure sensor for harsh environment," *Sensors and Actuators A: Physical*, vol. 197, pp. 30–37, 2013.

[9] S. T. Sanders, P. T. Jenkins, and R. K. Hanson, "Diode laser sensor system for multi-parameter measurements in pulse detonation engine flows," *Power*, vol. 5, p. 7, 2000.

[10] R. G. Azevedo, D. G. Jones, A. V. Jog et al., "A SiC MEMS resonant strain sensor for harsh environment applications," *IEEE Sensors Journal*, vol. 7, no. 4, pp. 568–576, 2007.

[11] C. Zhan, Y. Zhu, S. Yin, and P. Ruffin, "Multi-parameter harsh environment sensing using asymmetric Bragg gratings inscribed by IR femtosecond irradiation," *Optical Fiber Technology*, vol. 13, no. 2, pp. 98–107, 2007.

[12] J. van den Broeke, G. Langergraber, and A. Weingartner, "On-line and in-situ UV/vis spectroscopy for multi-parameter measurements: a brief review," *Spectroscopy Europe*, vol. 18, no. 4, pp. 15–18, 2006.

[13] M. A. Fonseca, J. M. English, M. von Arx, and M. G. Allen, "Wireless micromachined ceramic pressure sensor for high-temperature applications," *Journal of Microelectromechanical Systems*, vol. 11, no. 4, pp. 337–343, 2002.

[14] Y. Wang, Y. Jia, Q. Chen, and Y. Wang, "A passive wireless temperature sensor for harsh environment applications," *Sensors*, vol. 8, no. 12, pp. 7982–7995, 2008.

[15] M. A. Fonseca, *Polymer/ceramic wireless MEMS pressure sensors for harsh environments: high temperature and biomedical applications [Ph.D. thesis]*, Georgia Institute of Technology, 2007.

[16] Q. Tan, T. Luo, J. Xiong et al., "A harsh environment-oriented wireless passive temperature sensor realized by LTCC technology," *Sensors*, vol. 14, no. 3, pp. 4154–4166, 2014.

[17] M. A. Fonseca, *Polymer/Ceramic Wireless MEMS Pressure Sensors for Harsh Environments: High Temperature and Biomedical Applications*, Georgia Institute of Technology, Atlanta, Ga, USA, 2007.

[18] C. Zhang, J.-Q. Huang, and Q.-A. Huang, "Design of LC-type passive wireless multi-parameter sensor," in *Proceedings of the 8th Annual IEEE International Conference on Nano/Micro Engineered and Molecular Systems (NEMS '13)*, pp. 256–259, IEEE, April 2013.

[19] C. M. Zierhofer and E. S. Hochmair, "Geometric approach for coupling enhancement of magnetically coupled coils," *IEEE Transactions on Biomedical Engineering*, vol. 43, no. 7, pp. 708–714, 1996.

[20] S. Babic and C. Akyel, "Improvement in calculation of the self- and mutual inductance of thin-wall solenoids and disk coils," *IEEE Transactions on Magnetics*, vol. 36, no. 4, pp. 1970–1975, 2000.

[21] C. Akyel, S. I. Babic, and M.-M. Mahmoudi, "Mutual inductance calculation for noncoaxial circular air coils with parallel axes," *Progress in Electromagnetics Research*, vol. 91, pp. 287–301, 2009.

[22] M. Soma, D. C. Galbraith, and R. L. White, "Radio-frequency coils in implantable devices: misalignment analysis and design procedure," *IEEE Transactions on Biomedical Engineering*, vol. 34, no. 4, pp. 276–282, 1987.